NATIONAL RADIO ASTRONOMY OBSERVATORY
Green Bank, West Virginia

Electronics Division Internal Report No. 83

POINTING AND CALIBRATION WITH THE 300-FOOT FOUR-FEED SYSTEM

M. Felli and E. Churchwell

February 1969

NUMBER OF COPIES: 100

POINTING AND CALIBRATION WITH THE 300-FOOT FOUR-FEED SYSTEM

M. Felli and E. Churchwell

INTRODUCTION

Toward the end of December 1968 a survey of the 1400 MHz continuum emission of a selected list of Sharpless H II regions was started with the 300-foot transit telescope of the National Radio Astronomy Observatory. In order to reduce the time of observations required to map extended sources with a transit telescope, a four-feed system was used, which has been described by M. Davis and M. Hagstrom, Electronics Division Internal Report No. 68.

The beam positions and offsets were so chosen that an area of 35' in declination could be surveyed in a four-day period with a quarter beam separation. Four identical receivers were connected to the four feeds and were calibrated with the same noise source through directional couplers. In the following we describe the means by which the various parameters of the four-feed radio telescope have been derived. Radio source values are from the K. Kellermann-I. Pauliny-Toth catalog.

POINTING

A four-day program was necessary to determine the required parameters. On the first day 20' wobbles were made around the estimated position of the source with the two northern beams, the wobbling rate was 2.5°/min; the interval of 20' was chosen so that the source would pass through both beams and at the same time we would have at least four transits of each source. The peak position of the source in declination was measured from the analog records with an accuracy of $\pm$ 0!33. On the second day the same procedure was used for the two southern beams.

On the third day the Dec. values derived for the two northerm beams were used to point the telescope in Dec. so that the source would first scan through the peak position of the NE beam, then, after the source had moved half way between the NE and NW beams, as estimated from the wobble records, the antenna was moved to the Dec. of the peak position of the NW beam, so that both R.A. scans were centered on the Dec. peak position of the source. A 30-second thermal calibration was taken before and after each R.A. scan. On the fourth day the same procedure was used for the two southern beams.

Thus, at the end of the four-day period the following information was derived for each beam and for each source: peak position and HPBW in Dec., peak position and HPBW in R.A., and $T_{A\ max}$. The sources used are listed in Table I. Care was taken to include only point sources.

By comparing the precessed coordinates of the sources with the observed ones, five pointing curves were derived, one for each beam and one for the derived center of the four-feed system, which was later used for pointing the telescope. The errors are due to measuring inaccuracies and to the uncertainty in the catalogued position.

Figure 1 shows the Dec. correction versus Dec. Error bars were calculated for the center curve only, since this is the curve of interest to the observer. The error in the other four curves are comparable to those of the center curve. One can see that the beam offsets in Dec. remains relatively constant with Dec., and that the same peculiar behaviour between Dec. = 0° and Dec. = 25° is apparent in all four beams. The dip present in this Dec. interval probably comes about because the southern feed support leg is almost vertical in this Dec. range causing an uneven distribution of the weight between the two supports. Also in the Dec. interval +30° to +40° there seems to be a plateau which we suggest may be due to flexure of the dish and feed support as the antenna moves to either side of the zenith.

Figure 2 shows the R.A. pointing correction. Here also error bars were calculated only for the center curve. From these curves it is apparent that the offsets of the four beams remain constant with Dec. where allowance for the secant (δ) factor is taken into account. The curve for the center of the system indicates that the telescope axis is not exactly aligned along the EW direction and also that the axis is inclined with respect to the horizontal plane. The curve can be represented rather accurately by the formula

$$\Delta\alpha = \sec\delta\ [a \sin(\phi-\delta) + b \cos(\phi-\delta) + c]$$

where δ is the source declination, ϕ is the latitude of the Observatory, a is the azimuth error, b is the level error, and c is the collimation error. Using the data from the curve we find the values a = 4!8 ± 0!2, b = 1!0 ± 0!1 and c = 0!5 ± 0!1, which implies that (a) the west end of the axis of rotation is 3.3 cm south of the EW line, and (b) the west end of the axis of rotation is 1.4 cm higher than the eastern end.

HPBW AND BEAM OFFSETS

The HPBW of each beam in the NS direction was determined from the analogue record of the wobbles and in the EW direction from the drift scans. While the HPBW in the EW direction is accurate within ± 0!3, the HPBW in the NS direction is affected by several errors, such as 1) widening of the beam due to the factor $\tau v = 0.075$, where v is the velocity of the scan and τ is the receiver time constant (this effect has not been corrected for), and

2) the difficulty of fitting a baseline when the wobbling interval is short enough that a source does not completely pass out of the beam before the antenna changes direction, resulting in no base line between the two peaks. No variation of the HPBW with declination was detected within the erors of observation, therefore only the average value and the RMS for each beam are given in Table II. The HPBW is somewhat larger than that of the old 20/40 cm front end. This is due to the larger feeds used in the four-feed system. The larger feeds also explain the smaller aperture efficiency (28% instead of 31%; see the next section).

Also for the beam offsets, as indicated in Figures 2 and 3, no variation with Dec. was noticed. The mean value of the relative beam offsets are listed in Table III. The meaning of the terms used are illustrated in Figure 3, which shows the four beams as seen on the sky. Table IV gives the beam offsets relative to the center of the system.

APERTURE EFFICIENCY

The aperture efficiency, η_A, is related to the maximum antenna temperature $T_{A\,max}$ of a point source whose flux is S_v through the relation

$$\eta_A = \frac{2k\, T_{A\,max}}{S_v\, \pi \left(\frac{d}{2}\right)^2}$$

where d is the physical diameter of the antenna.

$T_{A\,max}$ is given by the relation

$$T_{A\,max} = \left[D_{s\,max}/D_{cal}\right] T_{cal}$$

where $D_{s\,max}$ is the maximum deflection of the source, D_{cal} is the deflection caused by the calibration signal, and T_{cal} is the noise temperature of the calibration signal. T_{cal} was slightly different for each signal. The values, as measured on January 19, 1969, were as follows:

$$T_{cal}\ NW = 4.30° \pm 0.05$$

$$T_{cal}\ NE = 4.02° \pm 0.05$$

$$T_{cal}\ SW = 3.84° \pm 0.05$$

$$T_{cal}\ SE = 3.92° \pm 0.05$$

η_A is shown as a function of declination for each beam in Figures 4-7. Due to noise and to uncertainties in determining the baseline, there may be an error of as much as 3% in the peak of individual antenna temperature and therefore an uncertainty in the aperture efficiency of 3% since

$$\Delta\eta_A/\eta_A = \frac{\Delta T_{A\ max}}{T_{A\ max}}$$

From the η_A versus Dec. curves (one for each beam), it should be noted: 1) the shape of the curve for all beams is essentially the same; 2) the peak of η_A for the two northern beams occurs at Dec. $\sim$ 25°, whereas for the southern beams it occurs at Dec. $\sim$ 15°; and 3) within the error the maximum value η_A for each beam is the same, 28% $\pm$ 1%.

The sources used to determine the aperture efficiency are the subset of those listed in Table I, which are marked with an asterisk. It was found that sources having flux densities less than 2.0 f.u. gave scattered values for η_A, mainly due to errors in the base line determination. Therefore, only the sources with $S_v \geq 2.0$ f.u. were used. Considerable care was also taken to use only nonvariable sources. Four of the sources with $S_v \geq 2.0$ were not used because they gave systematically lower values for η_A. We suspect that either the fluxes for these sources are in error, or that they are variable, or a combination of both. The sources are: NRAO 274; 4C 31.38, 3C 268.4, and 3C 285.

Between the December 1968 and January 1969 observing periods, the four-feed box was taken down from the focal position because of receiver noise. A comparison of the pointing curves in December and January indicates that the pointing corrections are identical for the two periods. The possibility that the box had been slightly rotated with respect to the December position was also checked by comparing the beam offsets derived in December and January. Since the differences appear to be random and generally less than 30", we concluded that no rotation had occurred.

TABLE I

NRAO	640	3C 36	NRAO	3930	3C 268.4
	860			3960	*3C 270.1
	1040	*3C 67		4013	
	1050	*3C 68.1		4050	*3C 275.0
	1300	3C 82		4120	*3C 278
	1340			4180	
	1400	4C 32.14		4220	3C 285
	2742			4240	*3C 287
	2810	3C 193		4280	3C 288.1
	2870	3C 197		*4345	
	2980	*3C 205		4410	*3C 298
	3150	3C 215		4530	*3C 303.1
	3202			4670	3C 311
	3280	*3C 223		4780	*3C 319
	3340	*3C 227		4820	3C 323
	3420	3C 232		5010	*3C 336
	3470	*3C 237		5100	3C 342
	3510	3C 240		*5170	
	3570	*3C 244.1		5210	3C 350
	3630	*3C 249.1		5260	3C 356
	3740	4C 30.21		5380	3C 363
	3810	*3C 263		5440	4C 23.47
	3890	4C 31.8			

TABLE II

BEAM	NS HPBW	EW HPBW
NW	11!3 ± 0!6	10!6 ± 0!3
NE	11!2 ± 0!8	10!6 ± 0!7
SW	11!7 ± 0!8	10!6 ± 0!3
SE	11!2 ± 0!5	10!6 ± 0!5

TABLE III

BEAM OFFSETS

R NEW	25!1 ± 0!4
R SEW	25!2 ± 0!6
R WNS	1!7 ± 0!3
R ENS	1!9 ± 0!4
Δ NEW	4!8 ± 0!2
Δ SEW	4.7 ± 0.2
Δ WNS	19!1 ± 0!2
Δ ENS	19!1 ± 0!2

TABLE IV

BEAM OFFSETS FROM CENTER

	Dec.	R.A.
NE (4)	+11!9	-11!7
SE (1)	- 7!2	-13!5
NW (3)	+ 7!2	+13!5
SW (2)	-11!9	+11!7

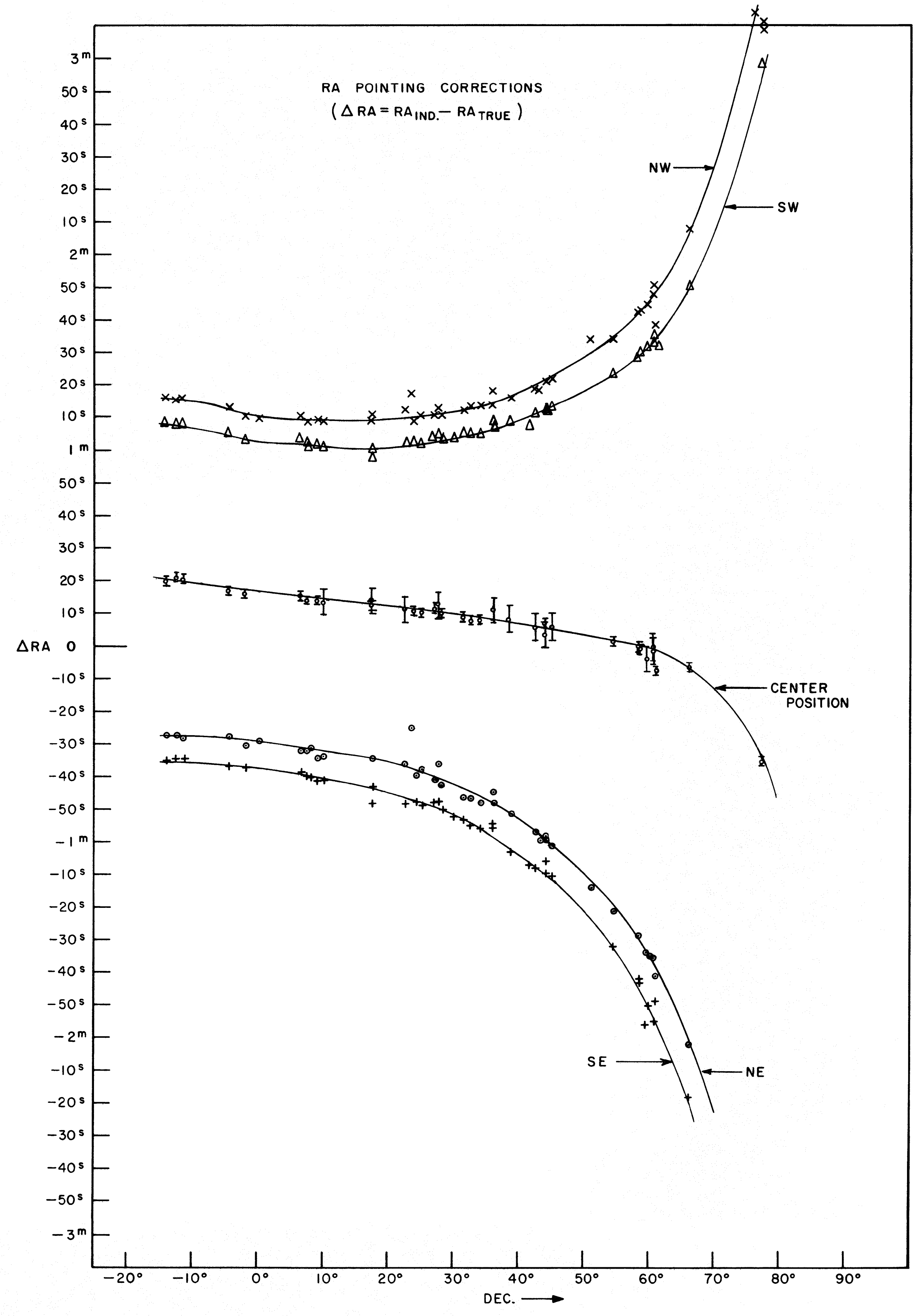
RA POINTING CORRECTIONS
(ΔRA = RA IND. − RA TRUE)
NW
SW
CENTER POSITION
SE
NE
ΔRA
DEC.

FIG. 2

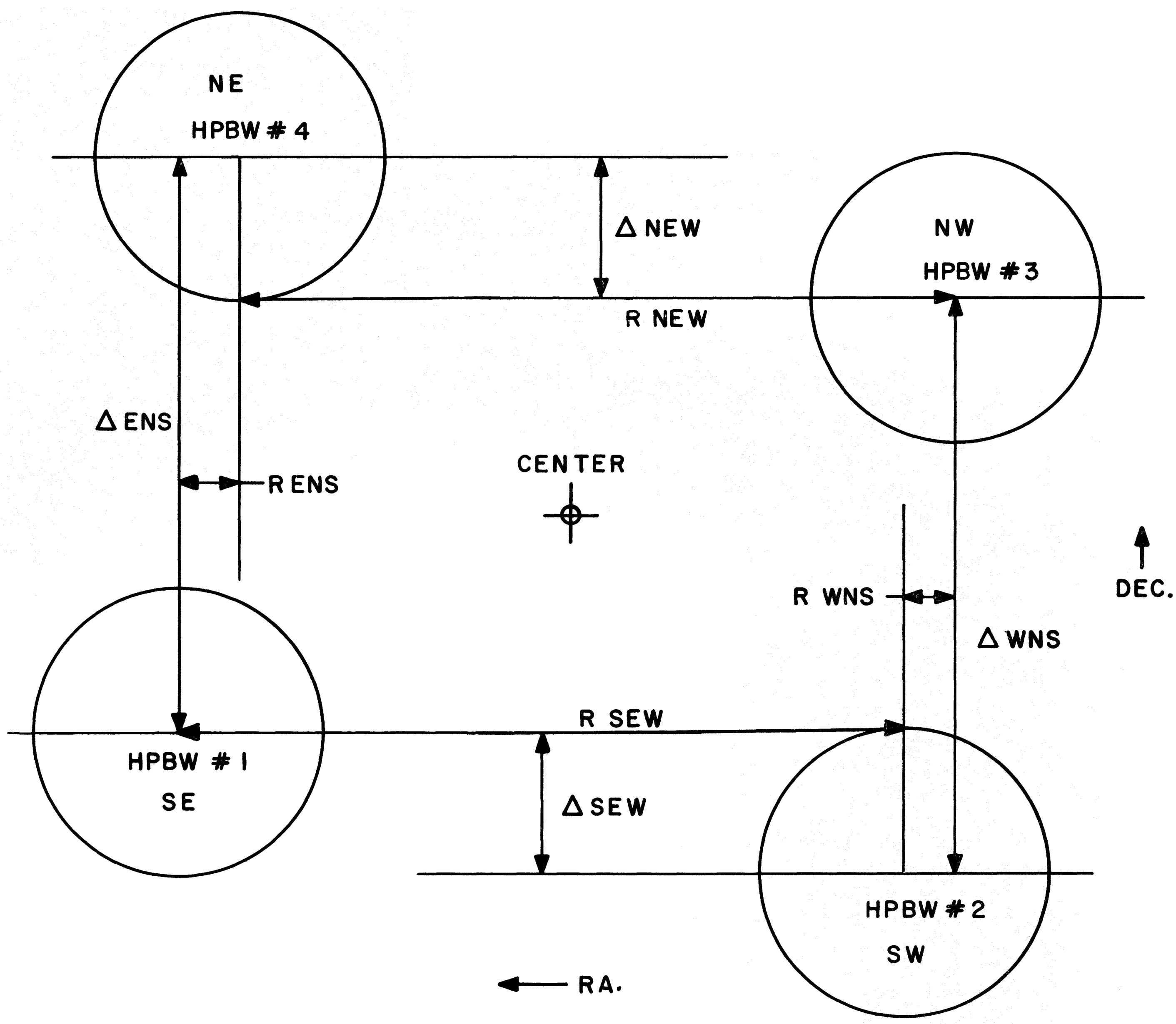

BEAM ORIENTATION ON THE SKY WITH OFFSETS LABELED AND EACH HPBW DRAWN TO SCALE.

FIG. 3

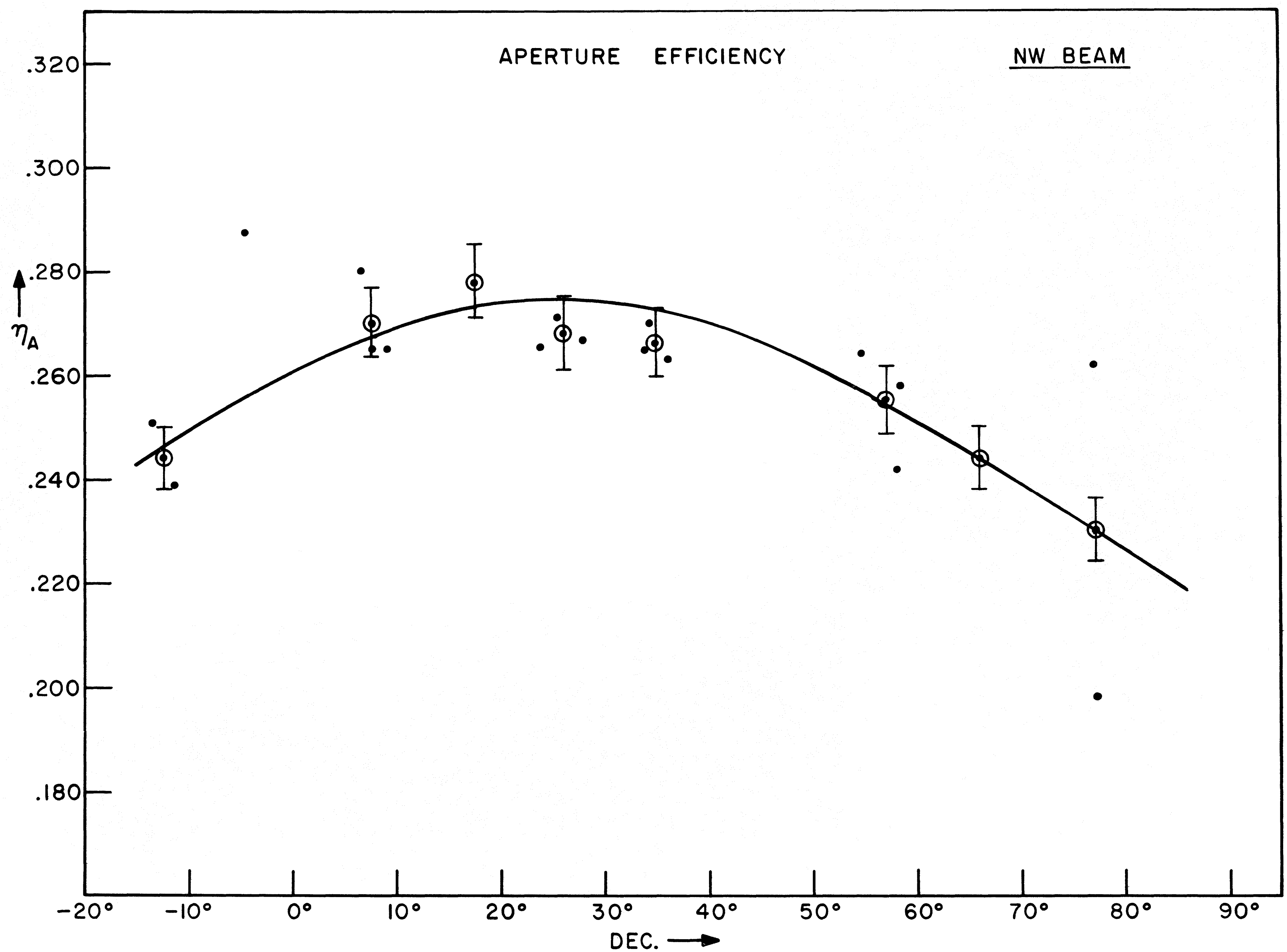
APERTURE EFFICIENCY
NW BEAM
.320
.300
.280
.260
.240
.220
.200
.180
η_A
-20°
-10°
0°
10°
20°
30°
40°
50°
60°
70°
80°
90°
DEC.

FIG. 4

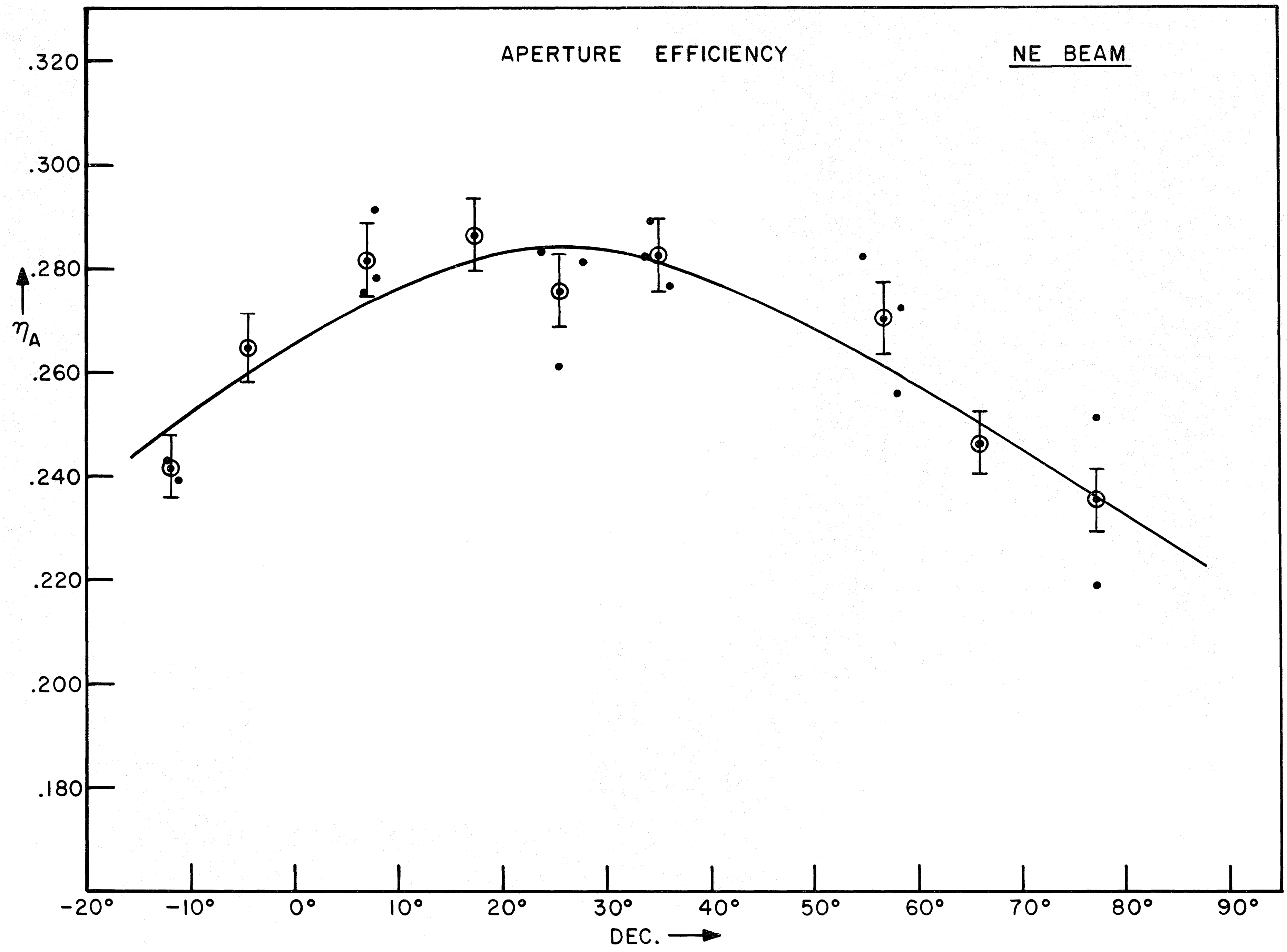

APERTURE EFFICIENCY
NE BEAM
.320
.300
.280
.260
.240
.220
.200
.180
η_A
-20°
-10°
0°
10°
20°
30°
40°
50°
60°
70°
80°
90°
DEC.

FIG. 5

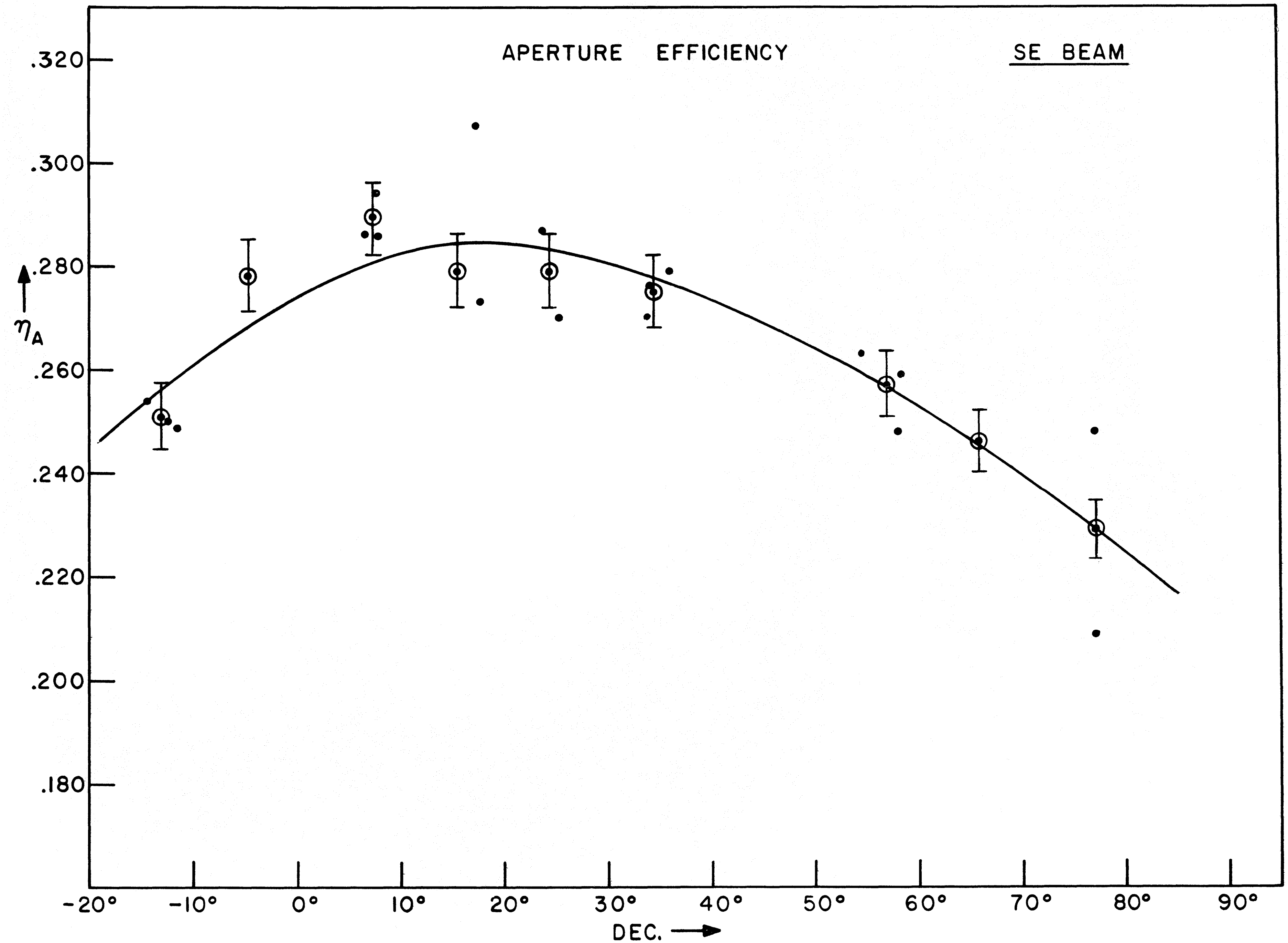
APERTURE EFFICIENCY
SE BEAM
.320
.300
.280
.260
.240
.220
.200
.180
η_A
-20°
-10°
0°
10°
20°
30°
40°
50°
60°
70°
80°
90°
DEC.

FIG 6

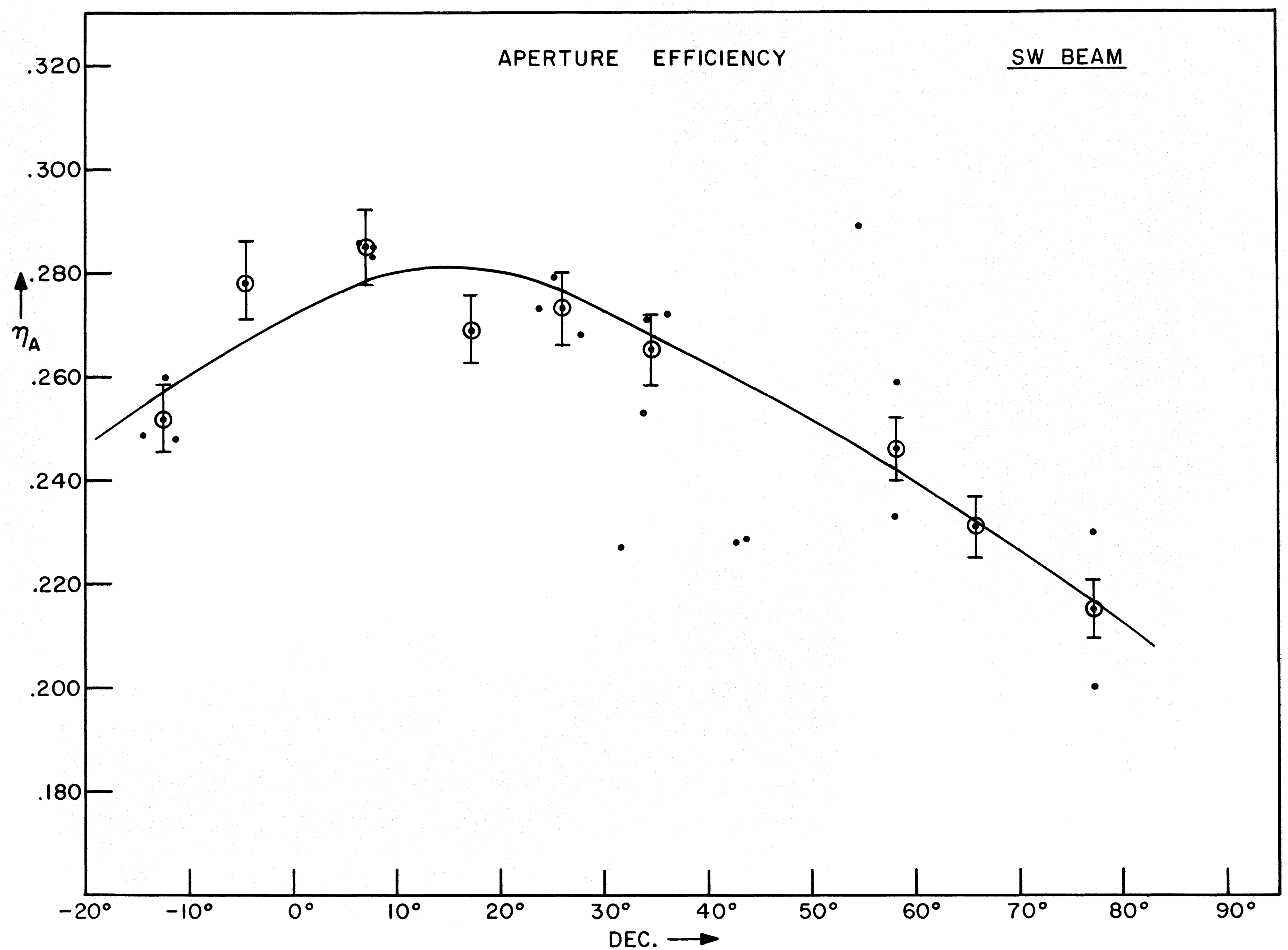
APERTURE EFFICIENCY
SW BEAM
η_A
.320
.300
.280
.260
.240
.220
.200
.180
-20°
-10°
0°
10°
20°
30°
40°
50°
60°
70°
80°
90°
DEC.

FIG. 7

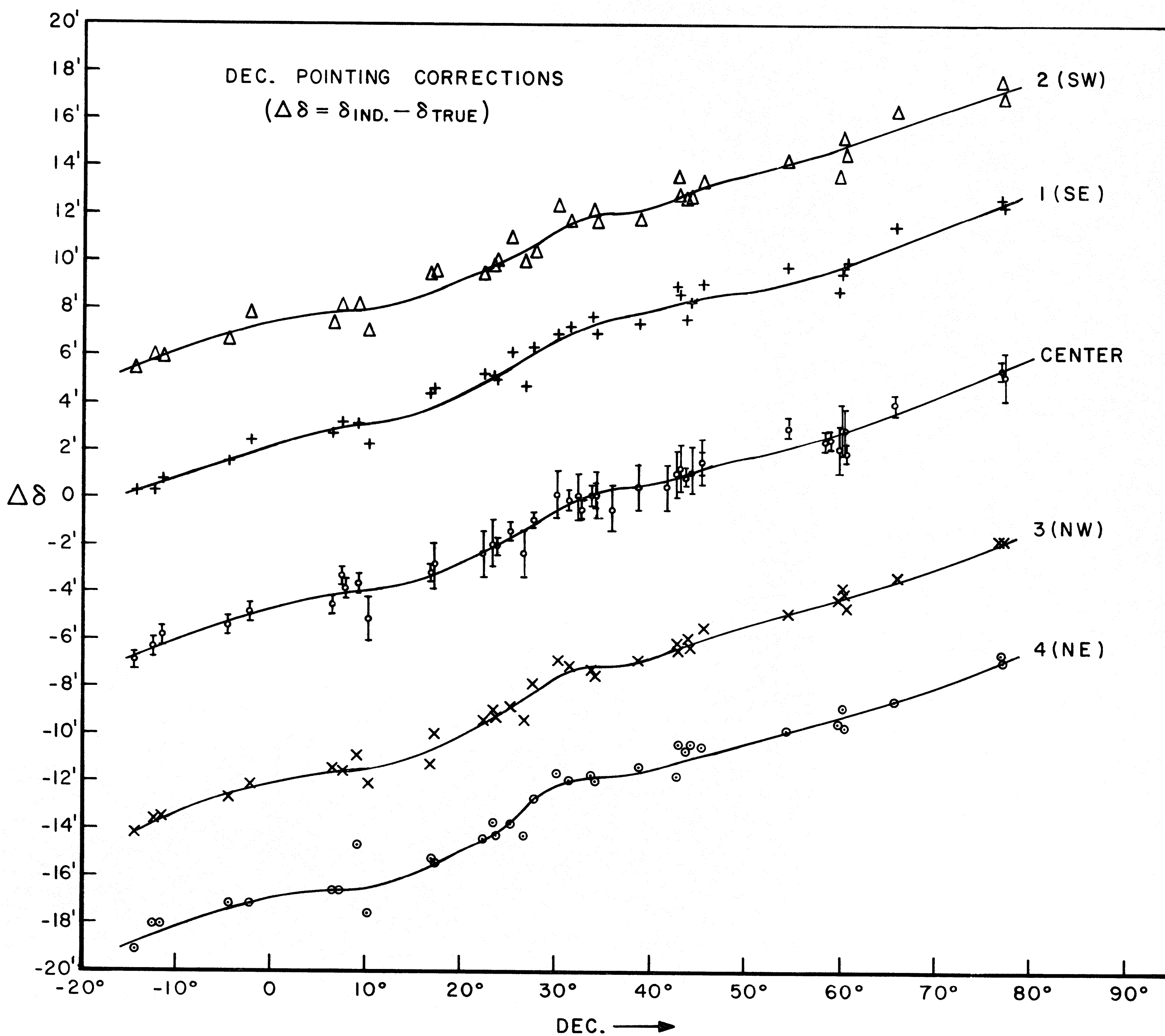

DEC. POINTING CORRECTIONS
($\Delta\delta = \delta_{IND.} - \delta_{TRUE}$)
2 (SW)
1 (SE)
CENTER
3 (NW)
4 (NE)
$\Delta\delta$
20'
18'
16'
14'
12'
10'
8'
6'
4'
2'
0
-2'
-4'
-6'
-8'
-10'
-12'
-14'
-16'
-18'
-20'
-20°
-10°
0
10°
20°
30°
40°
50°
60°
70°
80°
90°
DEC. →

FIG. 1